

FCNC Top Quark Production Via Anomalous Couplings

Elwin Martin¹ & Nikolaos Kidonakis²

¹Georgia Institute of Technology

²Kennesaw State University

August 16, 2013

Effective Lagrangians

Effective Lagrangians

$$\Delta\mathcal{L}_1 = \frac{1}{\Lambda} e \kappa_{tqV} \bar{t} \sigma_{\mu\nu} F_V^{\mu\nu} + h.c., \quad \Delta\mathcal{L}_2 = \frac{g_s \kappa_{qgt}}{\Lambda} \bar{t} \sigma^{\mu\nu} T^a \chi q G_{\mu\nu}^a + h.c.$$

where:

- Λ is an effective scale, e is the elementary charge and g_s is the strong coupling
- κ_{tqV} & κ_{tqq} are the anomalous couplings
- $\sigma_{\mu\nu} = \frac{i}{2} \gamma_{[\mu} \gamma_{\nu]}$ and γ_μ are the dirac matrices and T^a are the Gell-Mann matrices
- $\chi = f^L P_L + f^R P_R$ where $P_L(P_R)$ is the left(right) hand projection operator
- V is either a Z or a photon
- q is either a c or a u
- $F_V^{\mu\nu}$ is the field tensor for V , $G_{\mu\nu}^a$ is the field tensor for g

LHC as FCNC Probe

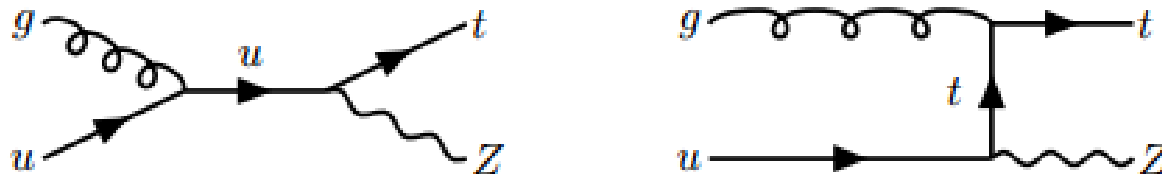
The LHC has been used to examine FCNC in the top-quark sector.

- Historically, HERA and Tevatron looked for these processes.
- ATLAS set limits of $\kappa_{ugt}/\Lambda < 6.9 \cdot 10^{-3} \text{TeV}^{-1}$ and $\kappa_{cgt}/\Lambda < 1.5 \cdot 10^{-2} \text{TeV}^{-1}$ and $\text{BR}(t \rightarrow Zq) < 0.73\%$ [Arxiv:1302.3698v1]
- We note that t - u - Z and t - u - γ dominate
- And charm contributions are small

Soft Gluon Corrections

Scale variations at LO produce large uncertainties, but higher order corrections stabilize the cross sections.

- Soft gluons important since the virtual and real diagrams don't cancel completely
- We define $s_4 = s + t + u - \sum m^2$ and $s_4 \rightarrow 0$ threshold
- We consider logarithmic corrections $\left[\frac{\ln^l(s_4/m^2)}{s_4} \right]_+$
- For α_s^n , LL $l = 2n - 1$ and NLL $l = 2n - 2$
- We calculate NLO at NLL

$gu \rightarrow tZ$ - DiagramFigure 1 : Tree level diagrams for $gu \rightarrow tZ$

$$g(p_g) + u(p_u) \rightarrow t(p_t) + Z(p_Z)$$

$$s = (p_g + p_u)^2, \quad t = (p_g - p_t)^2, \quad u = (p_u - p_t)^2$$

$$s_4 = s + t + u - m^2 - m_Z^2$$

$gu \rightarrow tZ$ - LO

The Born cross section for $gu \rightarrow tZ$ is given by:

$$\begin{aligned} & \frac{d^2 \hat{\sigma}_B^{gu \rightarrow tZ}}{dt du} \\ &= \frac{2\pi\alpha\alpha_s\kappa_Z}{3m^2s^3(m^2-t^2)^2} \{ 2m^8 - m^6(2m_Z^2 + 4s + 2t) \\ & - t [2m_Z^6 - 2m_Z^4(s+t) - 4st(s+t) + m_Z^2(s+t)] \\ & + m^4 [2m_Z^4 - m_Z(2s+t) + 2(s^2 + 4st + t^2)] \\ & + m^2 [2m_Z^6 - 4m_Z^4t + m_Z^2(s+t)(s+5t) - 2t(2s^2 + 6t + t^2)] \} \end{aligned}$$

$gu \rightarrow tZ$ - NLO

The NLO-NLL partonic cross section is given by:

$$\frac{d^2\hat{\sigma}_{gu \rightarrow tZ}^{(1)}}{dtdu} = F_B^{gu \rightarrow tZ} \frac{\alpha_s(\mu_R^2)}{\pi} \left(c_3 \left[\frac{\ln(s_4/m^2)}{s_4} \right]_+ + c_2 \left[\frac{1}{s_4} \right]_+ + c_1 \delta(s_4) \right)$$

where

$$c_1 = \left[C_F \ln \left(\frac{-t + m_Z^2}{m^2} \right) + C_A \ln \left(\frac{-u + m_Z^2}{m^2} \right) - \frac{3}{4} C_F - \frac{\beta_0}{4} \right] \ln \left(\frac{\mu_F^2}{m^2} \right) + \frac{\beta_0}{4} \ln \left(\frac{\mu_R^2}{m^2} \right)$$

$$c_2 = 2\text{Re}\Gamma_S^{(1)} - C_F - C_A - 2C_F \ln \left(\frac{-t + m_Z^2}{m^2} \right) - 2C_A \ln \left(\frac{-u + m_Z^2}{m^2} \right) - (C_F + C_A) \ln \left(\frac{\mu_F^2}{s} \right)$$

$$c_3 = 2(C_F + C_A)$$

and $C_F = (N_c^2 - 1)/(2N_c)$, $C_A = N_c$, $\beta_0 = (11C_A - 2n_f)/3$.

n_f is the number of light quark flavors and N_c the number of colors

$gu \rightarrow tZ$ - NNLO

The NNLO-NLL partonic cross section is given by:

$$\begin{aligned}
 \frac{d^2 \hat{\sigma}_{gu \rightarrow tZ}^{(2)}}{dt du} = & F_B^{gu \rightarrow tZ} \frac{\alpha_s^2(\mu_R^2)}{\pi^2} \left\{ \frac{1}{2} (c_3^{gu \rightarrow tZ})^2 \left[\frac{\ln^3(s_4/m^2)}{s_4} \right]_+ \right. \\
 & + \left[\frac{3}{2} c_3^{gu \rightarrow tZ} c_2^{gu \rightarrow tZ} - \frac{\beta_0}{4} c_3^{gu \rightarrow tZ} \right] \left[\frac{\ln^2(s_4/m^2)}{s_4} \right]_+ \\
 & + \left[c_3^{gu \rightarrow tZ} c_1^{gu \rightarrow tZ} + (C_F + C_A)^2 \ln^2 \left(\frac{\mu_F^2}{m^2} \right) - 2(C_F + C_A) T_2^{gu \rightarrow tZ} \ln \left(\frac{\mu_F^2}{m^2} \right) \right. \\
 & \quad \left. + \frac{\beta_0}{4} c_3^{gu \rightarrow tZ} \ln \left(\frac{\mu_R^2}{m^2} \right) - \zeta_2 (c_3^{gu \rightarrow tZ})^2 \right] \left[\frac{\ln(s_4/m^2)}{s_4} \right]_+ \\
 & + \left[-(C_F + C_A) \ln \left(\frac{\mu_F^2}{m^2} \right) c_1^{gu \rightarrow tZ} - \frac{\beta_0}{4} (C_F + C_A) \ln \left(\frac{\mu_F^2}{m^2} \right) \ln \left(\frac{\mu_R^2}{m^2} \right) \right. \\
 & \quad \left. + (C_F + C_A) \frac{\beta_0}{8} \ln^2 \left(\frac{\mu_F^2}{m^2} \right) - \zeta_2 c_2^{gu \rightarrow tZ} c_3^{gu \rightarrow tZ} + \zeta_3 (c_3^{gu \rightarrow tZ})^2 \right] \left[\frac{1}{s_4} \right]_+ \left. \right\}
 \end{aligned}$$

Figure 2 : $\sqrt{s} = 7$ where the ζ s are the Riemann zeta function of the subscript.

$pp \rightarrow tZ$ - Hadronic Cross Section

The partonic cross sections for NLO(1) and NNLO(2), $\frac{d^2\sigma^{(1,2)}}{dtdu}$, convolute into the hadronic cross sections by:

$$\sigma_{pp \rightarrow tZ}^{FCNC} = \int_{T_{min}}^{T_{max}} dT \int_{-S-T+m^2+m_Z^2}^{m^2+m^2S/(T-m^2)} dU \int_{(m_Z^2-T)/(S+U-m^2)}^1 dx_b \int_0^{x_b(S+U-m^2)+T-m_Z^2} ds_4$$

$$\times \frac{x_a x_b}{x_b S + T - m^2} \phi(x_a) \phi(x_b) \frac{d^2 \hat{\sigma}_{gu \rightarrow tZ}^{(1,2)}}{dtdu}$$

where T , S , and U are the Mandelstam variables for the hadronic process.

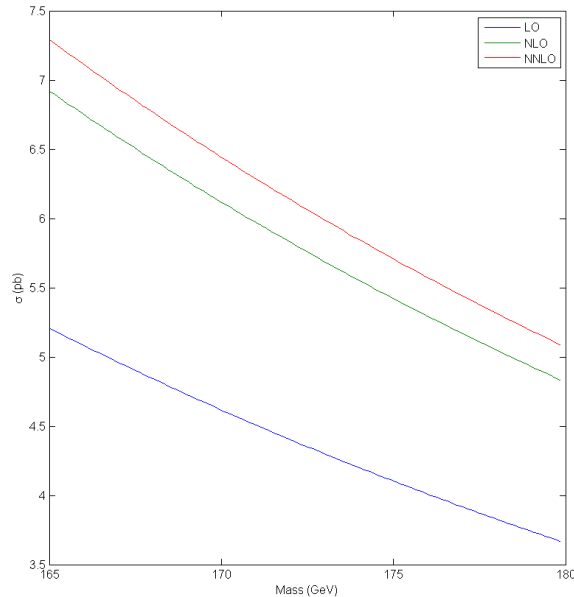
σ vs. m at 7 TeV

Figure 3 : $\sqrt{s} = 7$ TeV cross section for $gu \rightarrow tZ$ as a function of mass.

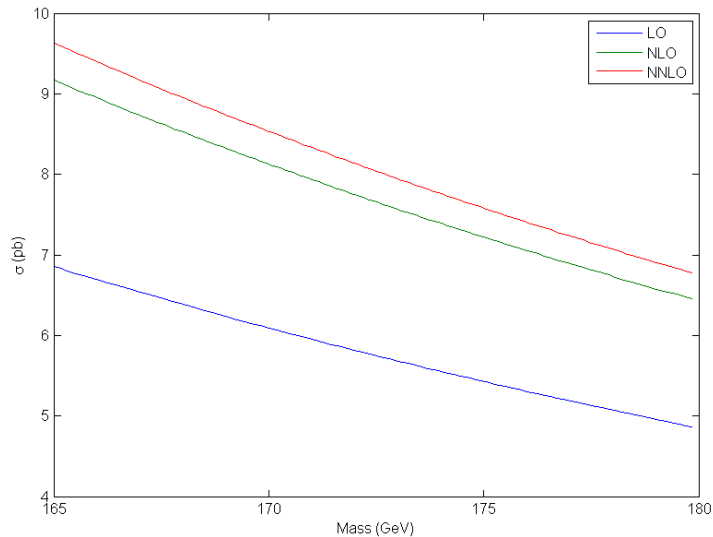
σ vs. m at 8 TeV

Figure 4 : $\sqrt{s} = 8$ TeV cross section for $gu \rightarrow tZ$ as a function of mass.

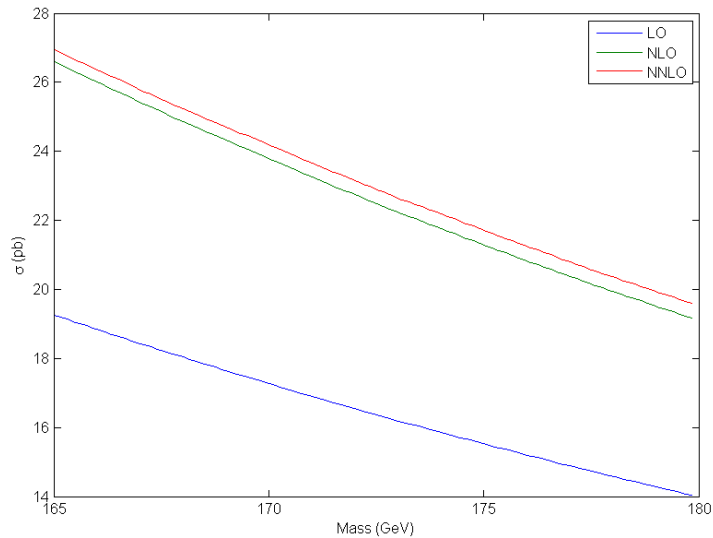
σ vs. m at 14 TeV

Figure 5 : $\sqrt{s} = 14$ TeV cross section for $gu \rightarrow tZ$ as a function of mass.

σ vs. m at NNLO for 7, 8, & 14 TeV

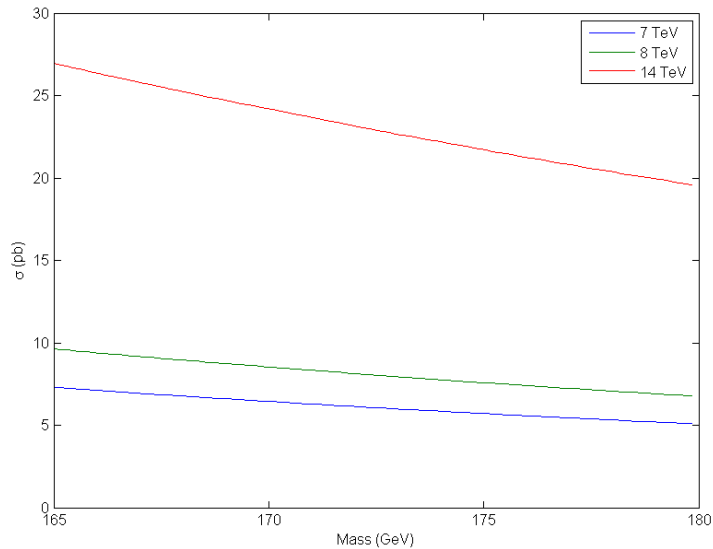


Figure 6 : $\sqrt{s} = 7, 8, \text{ \& } 14$ TeV cross sections for $gu \rightarrow tZ$ as a function of mass.

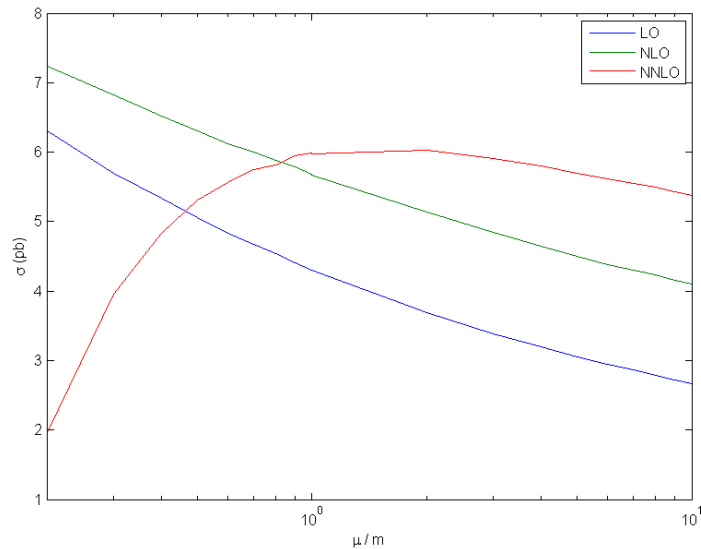
σ vs. μ at 7 TeV

Figure 7 : $\sqrt{s} = 7$ TeV cross section for $gu \rightarrow tZ$ scale dependence.

σ vs. μ at 8 TeV

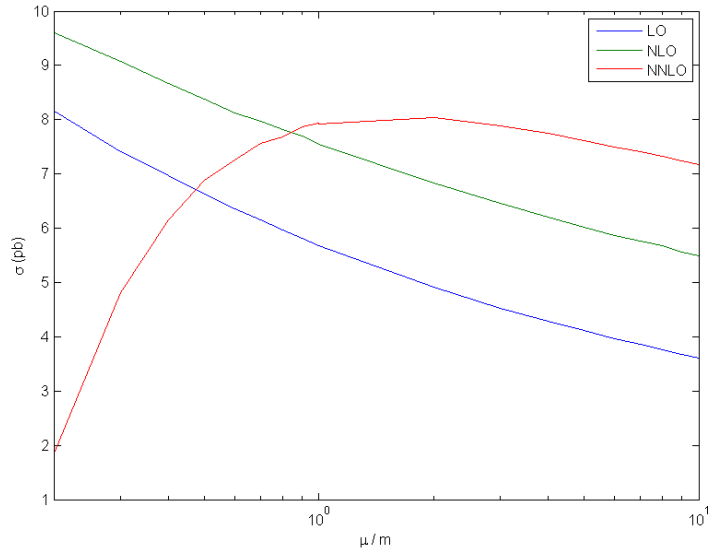


Figure 8 : $\sqrt{s} = 8$ TeV cross section for $gu \rightarrow tZ$ scale dependence.

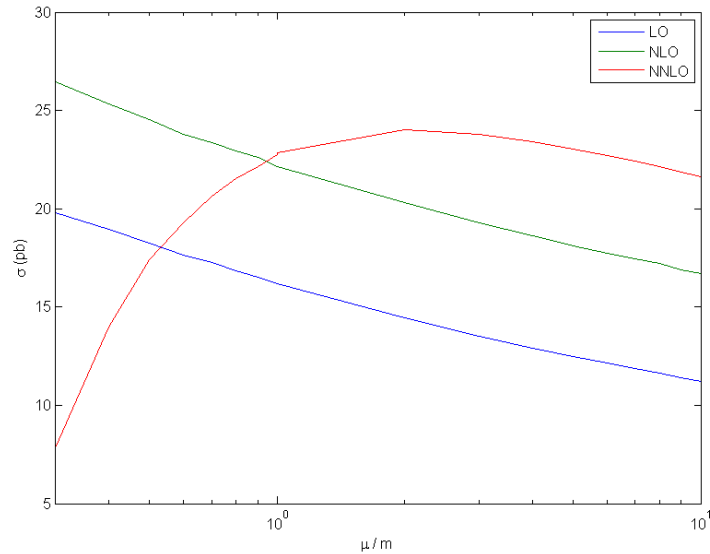
σ vs. μ at 14 TeV

Figure 9 : $\sqrt{s} = 14$ TeV cross section for $gu \rightarrow tZ$ scale dependence.

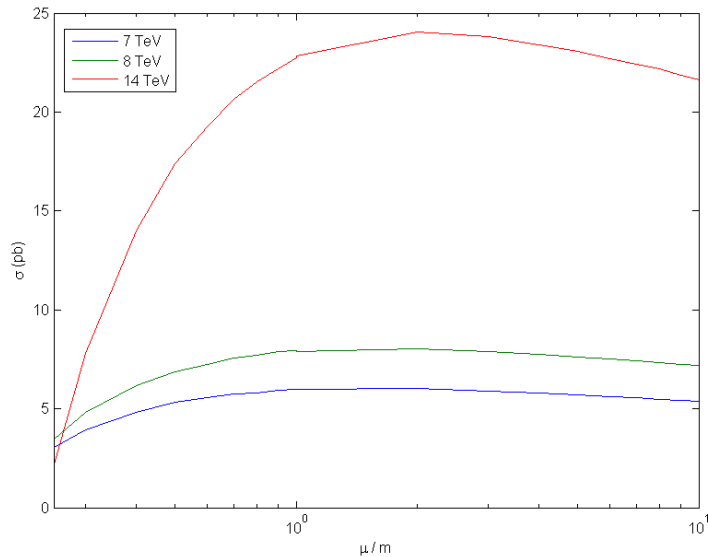
σ vs. μ at NNLO for 7,8, & 14 TeV

Figure 10 : $\sqrt{s} = 7, 8, \text{ \& } 14$ TeV cross sections for $gu \rightarrow tZ$ as a function of scale.

$gu \rightarrow t\gamma$ Figure 11 : Tree level diagrams for $gu \rightarrow t\gamma$

$$g(p_g) + u(p_u) \rightarrow t(p_t) + \gamma(p_\gamma)$$

$$s = (p_g + p_u)^2, \quad t = (p_g - p_t)^2, \quad u = (p_u - p_t)^2$$

$$s_4 = s + t + u - m^2$$

$gu \rightarrow t\gamma$ - LO

The Born cross section for $gu \rightarrow t\gamma$ is given by:

$$\frac{d^2 \hat{\sigma}_B^{gu \rightarrow t\gamma}}{dt du} = \frac{4\pi \alpha \alpha_s \kappa_\gamma (m^2 - s - t) [m^6 - m^4 s - 2st^2 + m^2 t(3s + t)]}{3m^2 s^3 (m^2 - t^2)^2} \delta(s_4)$$

where α & α_s are as noted above and $\kappa_\gamma = \kappa_{tg\gamma}$

$gu \rightarrow t\gamma$ - NLO

The NLO-NLL partonic cross section is given by:

$$\frac{d^2\hat{\sigma}_{gu\rightarrow t\gamma}^{(1)}}{dtdu} = F_B^{gu\rightarrow t\gamma} \frac{\alpha_s(\mu_R^2)}{\pi} \left(c_3 \left[\frac{\ln(s_4/m^2)}{s_4} \right]_+ + c_2 \left[\frac{1}{s_4} \right]_+ + c_1 \delta(s_4) \right)$$

where

$$c_1 = \left[C_F \ln \left(\frac{-t}{m^2} \right) + C_A \ln \left(\frac{-u}{m^2} \right) - \frac{3}{4} C_F - \frac{\beta_0}{4} \right] \ln \left(\frac{\mu_F^2}{m^2} \right) + \frac{\beta_0}{4} \ln \left(\frac{\mu_R^2}{m^2} \right)$$

$$c_2 = 2\text{Re}\Gamma_S^{(1)} - C_F - C_A - 2C_F \ln \left(\frac{-t}{m^2} \right) - 2C_A \ln \left(\frac{-u}{m^2} \right) - (C_F + C_A) \ln \left(\frac{\mu_F^2}{s} \right)$$

$$c_3 = 2(C_F + C_A)$$

Note that this is equivalent to the result for $gu \rightarrow tZ$ in the limit of $m_Z^2 \rightarrow 0$.

$pp \rightarrow t\gamma$ - Hadronic Cross Section

The partonic cross sections for NLO(1) and NNLO(2), $\frac{d^2\sigma^{(1,2)}}{dtdu}$, convolute into the hadronic cross sections by:

$$\sigma_{pp \rightarrow t\gamma}^{FCNC} = \int_0^{m^2-S} dT \int_{-S-T+m^2}^{m^2+m^2S/(T-m^2)} dU \int_{-T/(S+U-m^2)}^1 dx_b \int_0^{x_b(S+U-m^2)+T} ds_4$$

$$\times \frac{x_a x_b}{x_b S + T - m^2} \phi(x_a) \phi(x_b) \frac{d^2 \hat{\sigma}_{gu \rightarrow t\gamma}^{(1,2)}}{dtdu}$$

where T , S , and U are the Mandelstam variables for the hadronic process.

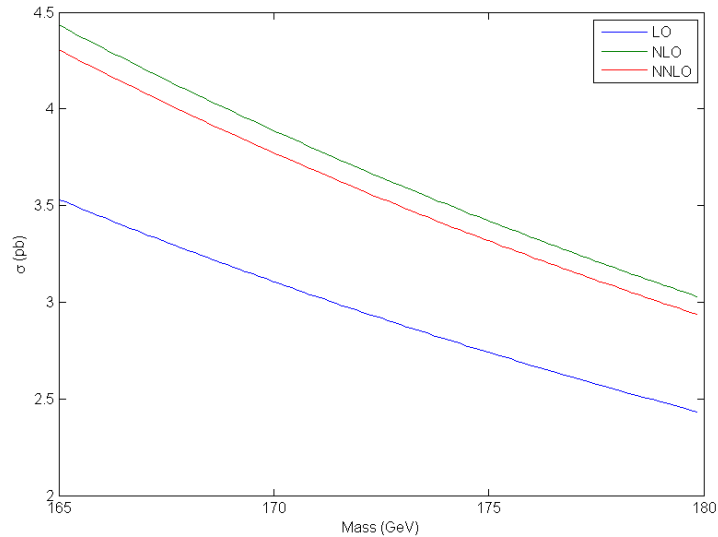
σ vs. m at 7 TeV

Figure 12 : $\sqrt{s} = 7$ TeV cross section for $gu \rightarrow t\gamma$ as a function of mass.

σ vs. m at 8 TeV

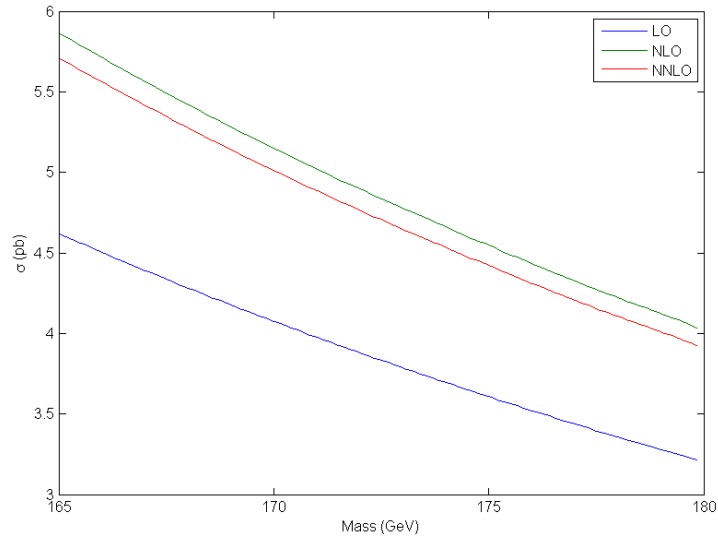


Figure 13 : $\sqrt{s} = 8$ TeV cross section for $gu \rightarrow t\gamma$ as a function of mass.

σ vs. m at 14 TeV

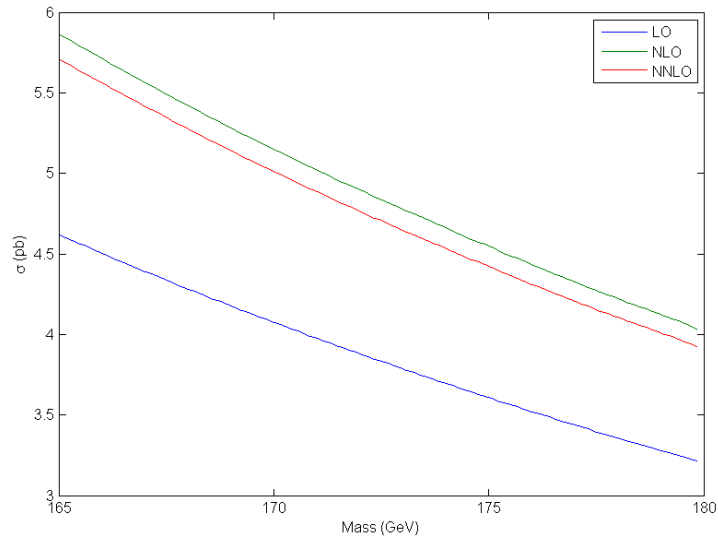


Figure 14 : $\sqrt{s} = 14\text{TeV}$ cross section for $gu \rightarrow t\gamma$ as a function of mass.

σ vs. m at NNLO for 7, 8, & 14 TeV

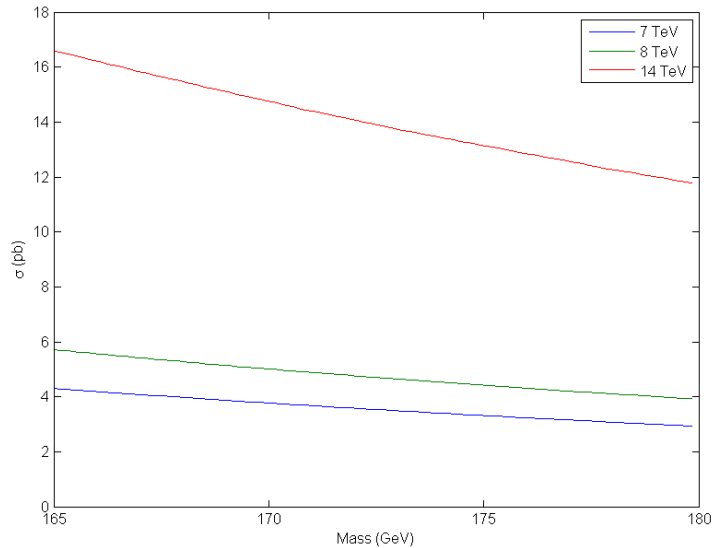


Figure 15 : $\sqrt{s} = 7, 8, \text{ \& } 14$ TeV cross sections for $gu \rightarrow t\gamma$ as a function of mass.

σ vs. μ at 7 TeV

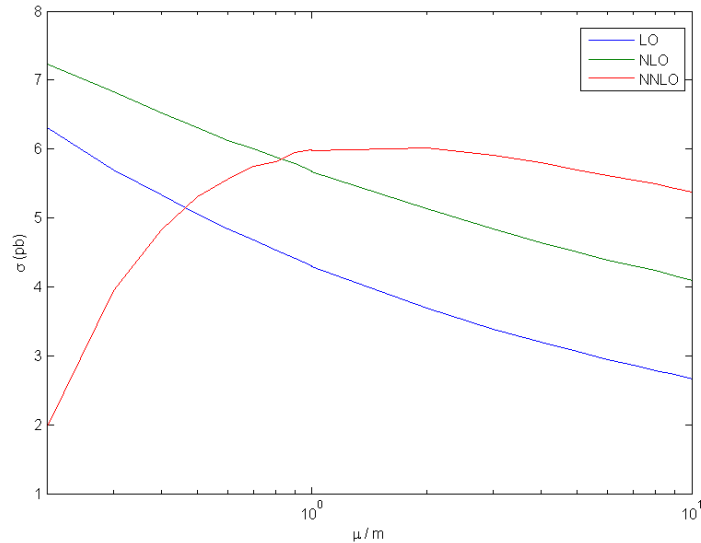


Figure 16 : $\sqrt{s} = 7$ TeV cross section for $gu \rightarrow t\gamma$ scale dependence.

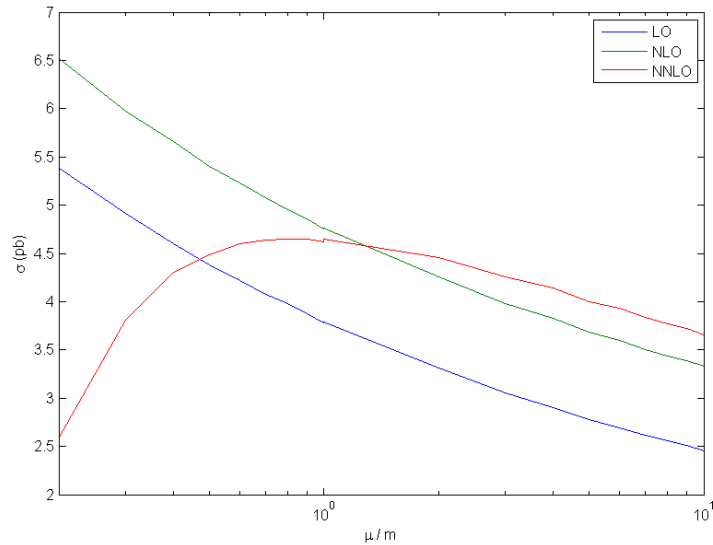
σ vs. μ at 8

Figure 17 : $\sqrt{s} = 8$ TeV cross section for $gu \rightarrow t\gamma$ scale dependence.

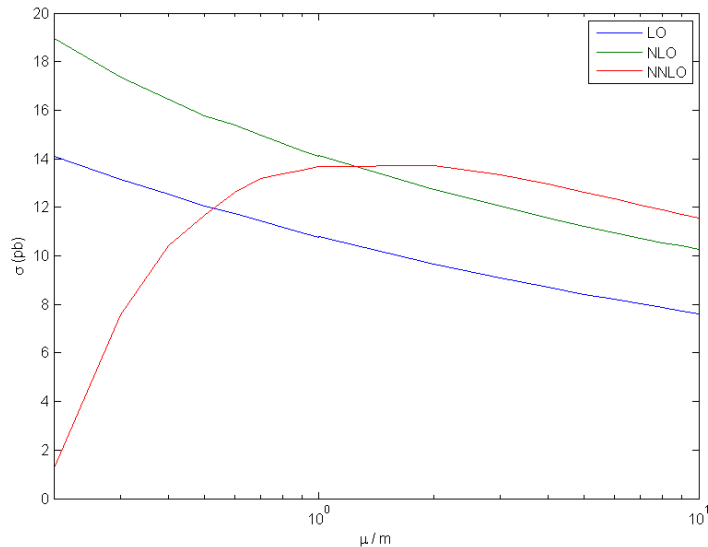
σ vs. μ at 14

Figure 18 : $\sqrt{s} = 14$ TeV cross section for $gu \rightarrow t\gamma$ scale dependence.

σ vs. μ at NNLO for 7,8, & 14 TeV

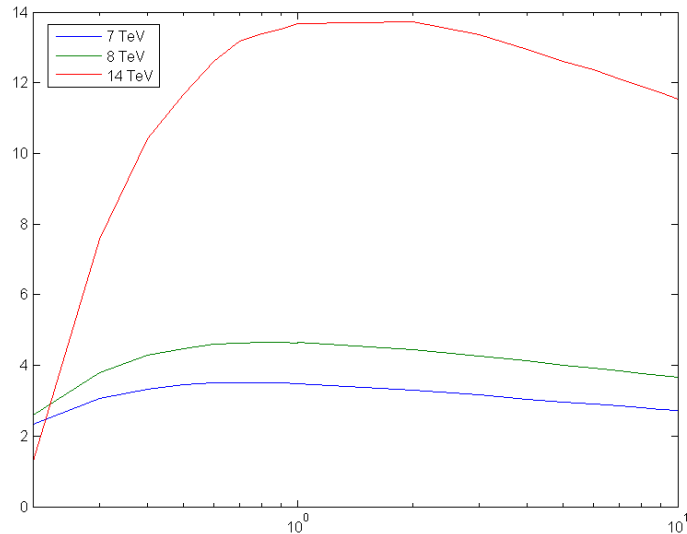


Figure 19 : $\sqrt{s} = 7, 8, \text{ \& } 14$ TeV cross sections for $gu \rightarrow t\gamma$ as a function of scale.

$gu \rightarrow tg$ - Tree Level Diagrams

Tree level diagrams
for $gu \rightarrow tg$

$$g(p_{g1}) + u(p_u)$$

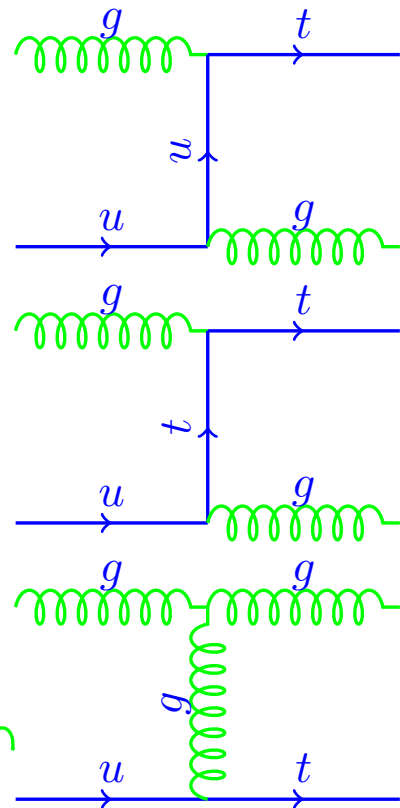
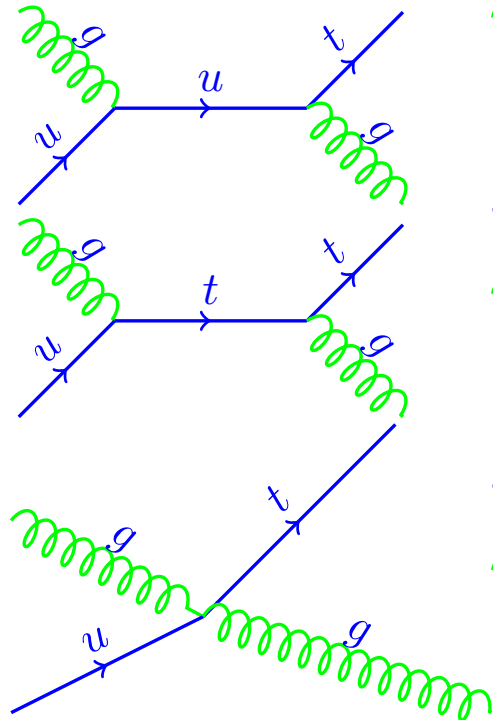
$$\rightarrow t(p_t) + g(p_{g2})$$

$$s = (p_{g1} + p_u)^2,$$

$$t = (p_{g1} - p_t)^2$$

$$u = (p_u - p_t)^2$$

$$s_4 = s + t + u - m^2$$

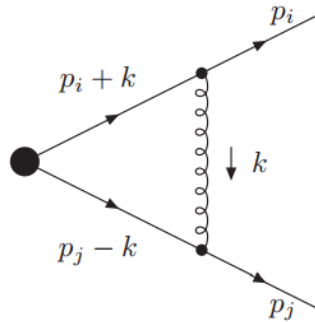


$gu \rightarrow tg$ - Progress

Still a work in progress

- Born cross section calculated...but not useable.
- Poles isolated...also not useable.
- Color factors calculated, actually useable!
- Conversion to meaningful representation and numerics to follow soon!

$gu \rightarrow tg$ - Example Pole Extraction



- 1. Apply Eikonal rules
- 2. Calculate diagram
- 3. ????
- 4. Profit!

$gu \rightarrow tg$ - Example Pole Extraction

Begin with the integral,

$$I_{exp} = g_s^2 \int \frac{d^n k}{(2\pi)^n} \frac{(-i)g^{\mu\nu}}{k^2} \frac{v_i^\mu}{v_i \cdot k} \frac{(-v_j^\nu)}{(-v_j \cdot k)}$$

Feynman parametrize,

$$= -2ig_s^2 \frac{v_i \cdot v_j}{(2\pi)^n} \int_0^1 dx \int_0^{1-x} dy \int \frac{d^n k}{(xk^2 + yv_i \cdot k + (1-x-y)v_j \cdot k)^3}$$

$gu \rightarrow tg$ - Example Pole Extraction (Cont.)

Integrate over k ,

$$I_{exp} = g_s^2 v_i \cdot v_j 2^{6-2n} \pi^{-n/2} \Gamma\left(3 - \frac{n}{2}\right) \int_0^1 x^{3-n} dx \int_0^{1-x} dy$$

$$\times \left(-y^2 v_i^2 - (1-x-y)^2 v_j^2 - 2y v_i \cdot v_j (1-x-y)\right)^{n/2-3}$$

and then take the other integrals in the $n = 4 - \epsilon$ limit and include the relevant kinematics

$$= -\frac{\alpha_s}{\pi} \ln\left(\frac{\sqrt{2} v_i \cdot v_j}{\sqrt{v_j^2}}\right) \frac{1}{\epsilon}$$

in the case where one of the outgoing quarks is massless

Summary & Conclusions

- We presented NNLO-NLL calculations for $pp \rightarrow tZ$ and $pp \rightarrow t\gamma$ at 7, 8, and 14 TeV
- We find that the corrections at NLO are large, mostly between 25% & 37%; NNLO corrections were on the order of \sim few%
- And scale dependence is only minimally improved by NLO, but is less pronounced at higher energies; NNLO scale dependence is bad at low scale factors, but evens out for around m and above.
- Our immediate next step will be the completion of the $gu \rightarrow tg$ cross section
- Afterwards? TBD

Acknowledgements



I would like to thank the Society of Physics Students for providing some of the funds for my travel. The rest of my funding was provided through NSF grant PHY 1212472.